

Electronic Supplementary Information

Construction nanocavity structure with carrier-selective layer for enhancement photocatalytic hydrogen production performance

Qin Lei¹, Rongzhi Chen^{1,2*}, Jihua Tan^{1*}, Xinxin Long¹, Huanyu Chen¹, Xinming Wang^{1,2}, Jingfu Liu^{1,3}, Zhongfang Lei⁴, Zhenya Zhang⁴

¹College of Resources and Environment, University of Chinese Academy of Sciences, Yuquan Road 19A, Beijing 100049, China

²State Key Laboratory of Organic Geochemistry and Guangdong Key Laboratory of Environmental Protection and Resources Utilization, Guangzhou Institute of Geochemistry, Chinese Academy of Sciences, Guangzhou 510640, China

³State Key Laboratory of Environmental Chemistry and Ecotoxicology, Research Center for Eco-Environmental Sciences, Chinese Academy of Sciences, Beijing 100085, China

⁴Graduate School of Life and Environmental Sciences, University of Tsukuba, 1-1-1 Tennodai, Tsukuba, Ibaraki 305-8572, Japan

*Corresponding author

Experimental section

Photodeposition and physical mixed Au/CdS NWs photocatalysts preparation.

The in-situ photodeposition 4% Au/CdS composite was prepared via photo reduction method.^{S1} In a typical process, a certain amount CdS powder was placed in 50 mL isopropanol aqueous solution (50%, v/v) in a photo reactor. A certain amount of HAuCl₄ (1%, wt/wt) aqueous solution was injected into the reactor sealed with a rubber septum. The reactor was purged with argon (Ar) gas for 30 min to remove oxygen. The mixture was irradiated by UV light under magnetic stirring for 2 h. Then, the solution was centrifuged, washed with distilled water and isopropanol to remove impurities, and obtained the samples after drying.

The physical mixed Au/CdS NWs samples were obtained by directly mixing CdS NWs and Au NPs (the average size is 11 nm) sol. The 11 nm Au NPs sol were prepared by a literature reported method. Typically, 0.5 mL HAuCl₄ (1%, wt/wt) were added into 50 mL deionized water, after the mixture solution were heated to 95 °C, 1.5 mL sodium citrate (1%, wt/wt) aqueous solution were injected, and continue the reaction for 20 min. The 11 nm Au NPs sol samples were obtained after centrifugal treatment, washing to obtain Au NPs sample. The morphology and UV-vis absorption of preparation Au NPs sol are shown in Fig. S17. The physical mixed 4% Au/CdS NWs samples were obtained by mixing the certain amount of Au NPs and CdS NWs.

The detection of Cd²⁺ concentration in residual solution after hydrothermal reaction. The residual Cd²⁺ in 2% Au and 10% Au system were detected by fluorescent spectrometry. The mechanism can be described as follow: the S²⁻ can reaction with Cd²⁺ to form CdS, which has a characteristic emission peak center at about 500-600 nm.^{S2} In a typically process, 0.5 mL supernatant solution after hydrothermal reaction was filtrated via organic membrane. Then, the obtained solution was diluted to 7 mL, excess Na₂S aqueous solution (0.1 mol·L⁻¹) were added under stirring condition, and continue stirring for 10 min. The measurements of PL spectra were carried out with a 460 nm light excitation and the results were presented in Fig. S7.

The calculation of photocatalyst band gap and band position. The band gap of

samples was transferred via K-M equation and the results were shown in Fig. S23a.^{S3} To study the band position of our photocatalysts, we subjected the CdS NWs and Au/CdS@Au-S composites electrode to measure flat band potential via electrochemical impedance-potential technique. The obtained Motte-Schottky plots are shown in Fig. S23b. Motte-Schottky plot of data analyzed using fitting method obeys Ref. S4. Above experiments were carried out in 0.1 mol·L⁻¹ H₂SO₄ solution at a fix frequency of 1000 Hz within the potential region of -1.5 to 1.5 V vs. Hg/HgCl₂ reference electrode. Variation of capacitance (C) with applied potential is shown by the Motte-Schottky equation (1):

$$\frac{1}{C^2} = \frac{2}{\varepsilon \cdot \varepsilon_0 \cdot e_0 \cdot A^2 \cdot N_D} \left(E - E_{FB} - \frac{kT}{e_0} \right) \quad (1)$$

where C is the space charge capacitance, ε and ε_0 are the permittivity of the electrode and free space, e_0 is the elementary charge, A is the electrochemical specific surface area, E is the applied potential, E_{FB} is the flat band potential, k is the Boltzmann's Constant and T is the temperature.

The positive slope of the plot confirms the n-type behavior of the CdS NWs and Au/CdS@Au-S composites, and the flat-band potentials of photocatalysts calculated from the x intercepts of the linear region, is 0.001 and -0.019 V vs. Hg/HgCl₂, respectively. Generally, the potential measured against an Hg/HgCl₂ reference can be converted into reversible hydrogen electrode (RHE) potentials by using Eq. (2):

$$E_{FB} \text{ (vs. RHE)} = E_{FB} \text{ (SCE)} + E_{SCE} + 0.059\text{pH} \quad (2)$$

The measured pH value of the electrolyte is approximately 1, and $E_{SCE}=0.24$ V. Therefore, the calculated flat-band positions of CdS NWs and Au/CdS@Au-S composites are 0.30 and 0.28 V vs. RHE (pH=0), respectively. Based on the results of band gap (Fig. S23a) and XPS valance results (Fig. S23c), thus, the corresponding conduction band (CB) and the valence band (VB) found at -0.35 and 2.05 V for CdS NWs, and -0.48 and 1.84 V for Au/CdS@Au-S vs. RHE, respectively (Fig. S23d).

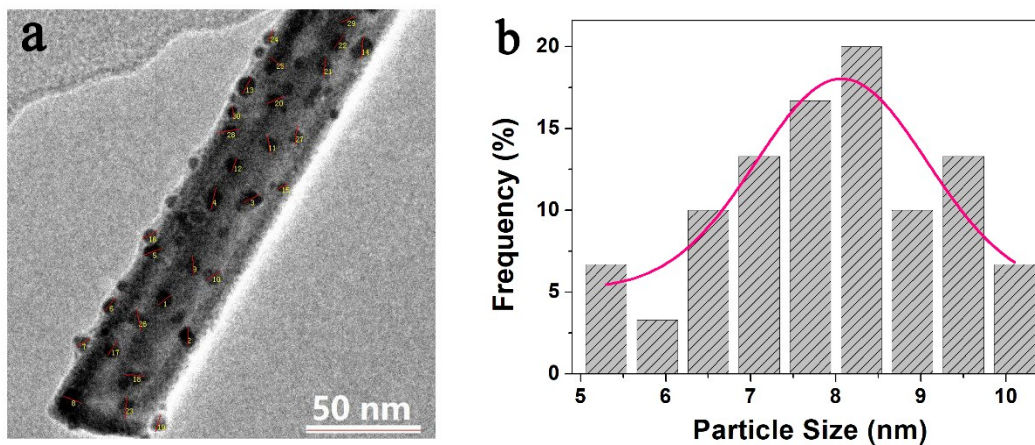


Fig. S1 The size statistics of Au NPs in Au/CdS@Au-S photocatalysts. (a) The statistic region, and (b) the result of size distribution.

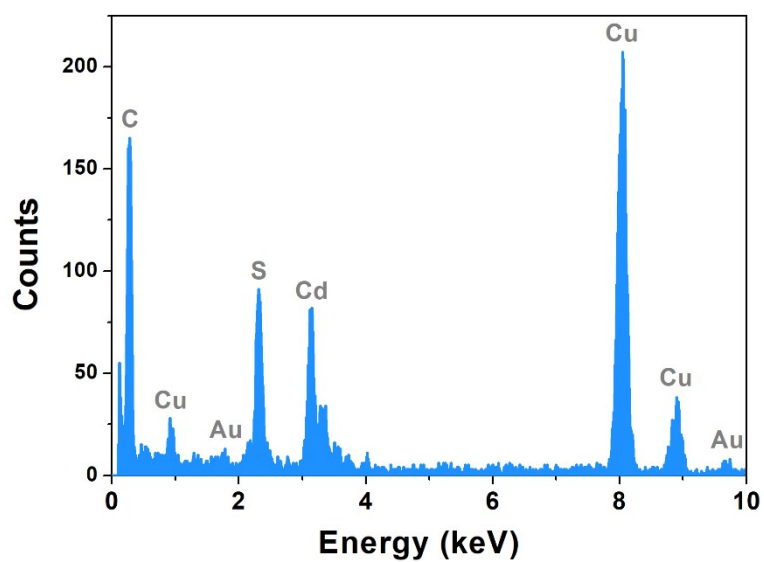


Fig. S2 The EDS of Au/CdS@Au-S photocatalysts.

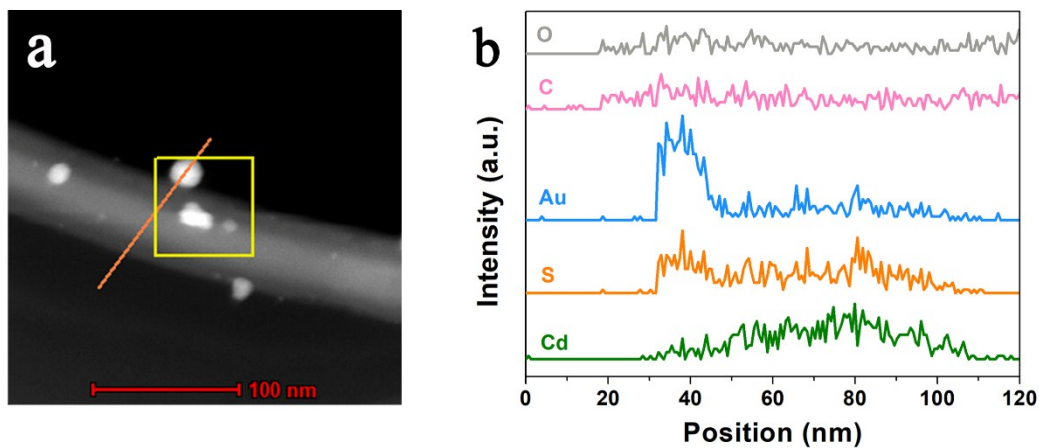


Fig. S3 The TEM linear sweep image of Au/CdS@Au-S photocatalysts. (a) The scanning area, and (b) the elements distribution at different position.

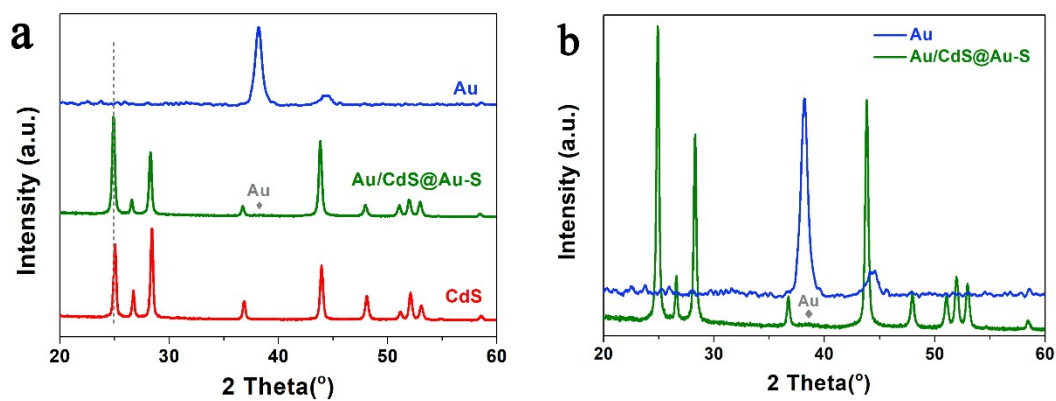


Fig. S4 (a) The XRD patterns of as-prepared samples and (b) the amplification patterns of Au and Au/CdS@Au-S.

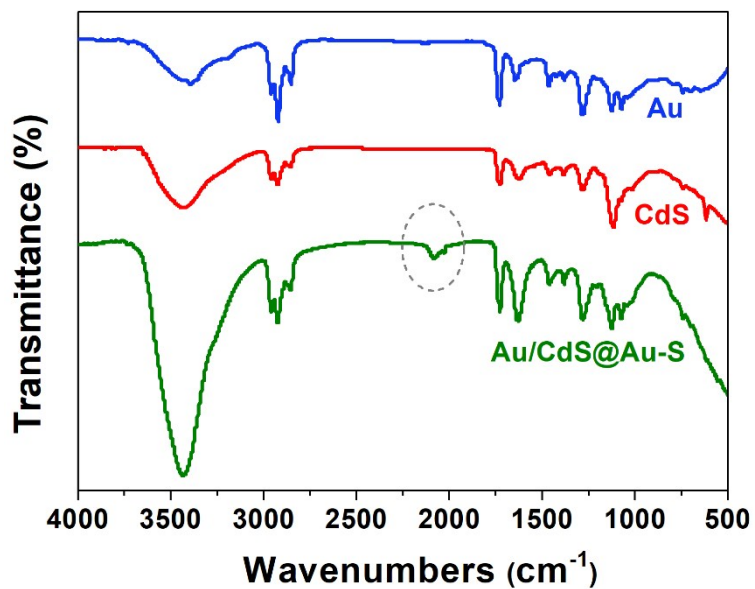


Fig. S5 The FTIR spectra of as-prepared CdS NWs, Au NPs and Au/CdS@Au-S samples.

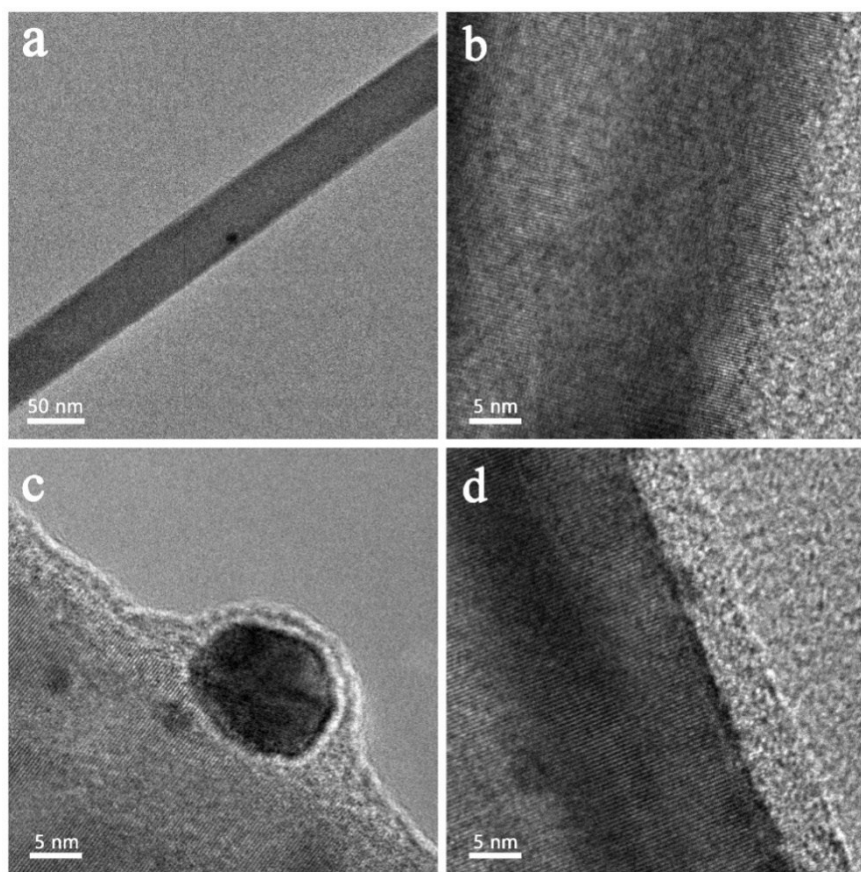


Fig. S6 The Au-S covering thickness change with the amount of HAuCl_4 at the Au addition of (a) 0.5%, (b) 0.5%, (c) 4% and (d) 10%, respectively.

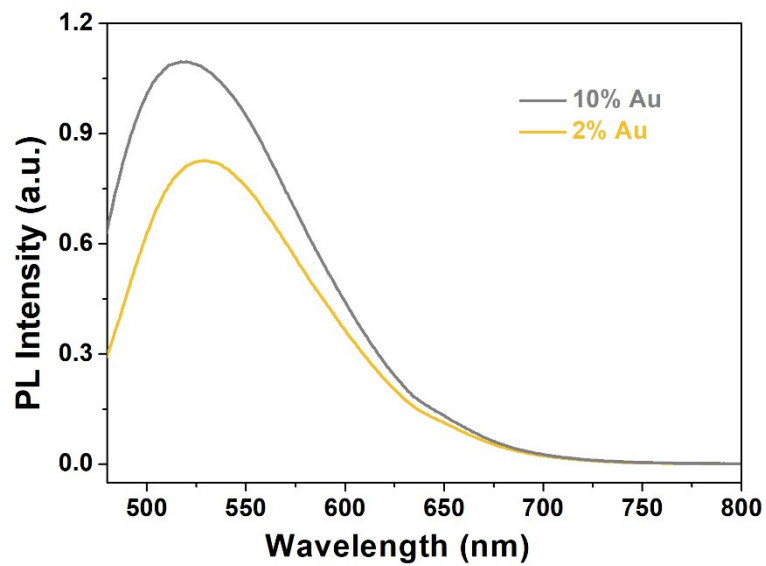


Fig. S7 The PL spectra of formed CdS with different hydrothermal reaction residual solution.

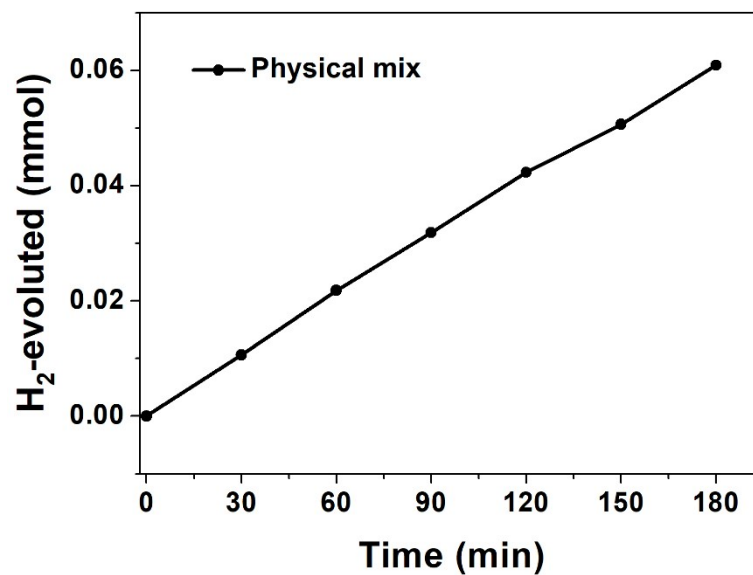


Fig. S8 Comparison in hydrogen evolution activity of Au/CdS NWs from different preparation methods.

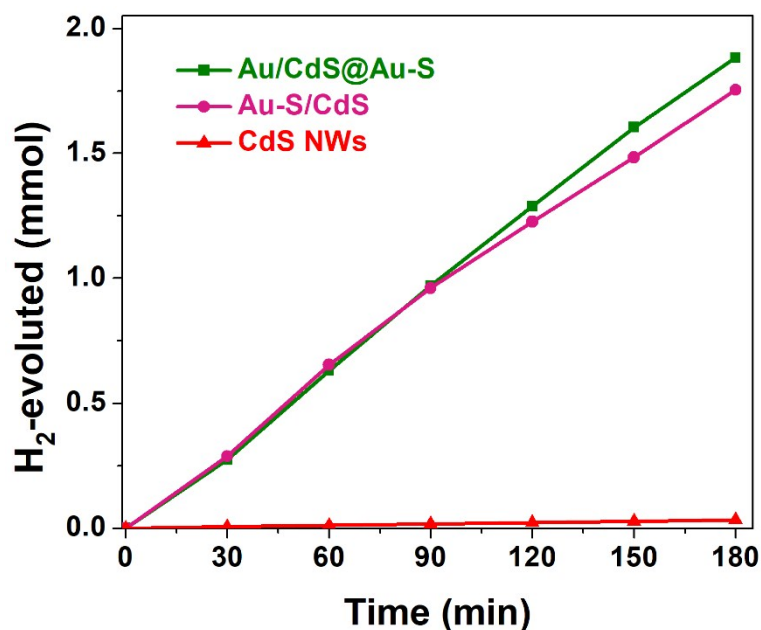


Fig. S9 The photocatalytic hydrogen production activity comparison on CdS, Au-S/CdS and Au/CdS@Au-S photocatalyst under the same condition.

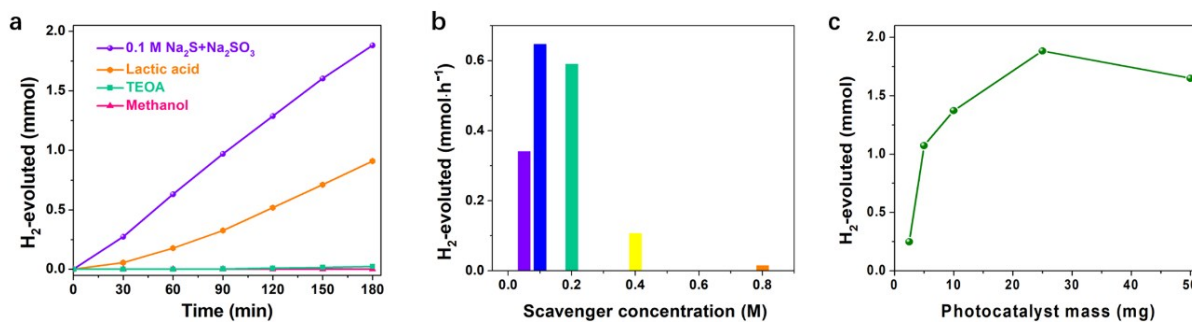


Fig. S10 (a) The photocatalytic hydrogen production activity over 25 mg Au/CdS@Au-S photocatalyst under various scavenger, the concentration of lactic acid, TEOA and methanol all is 10% (v/v), (b) the photocatalytic hydrogen production activity over 25 mg Au/CdS@Au-S photocatalyst at different concentrations of Na₂S and Na₂SO₃ (the concentration of Na₂S and Na₂SO₃ is the same) and (c) the relationship of hydrogen performance and photocatalyst mass.

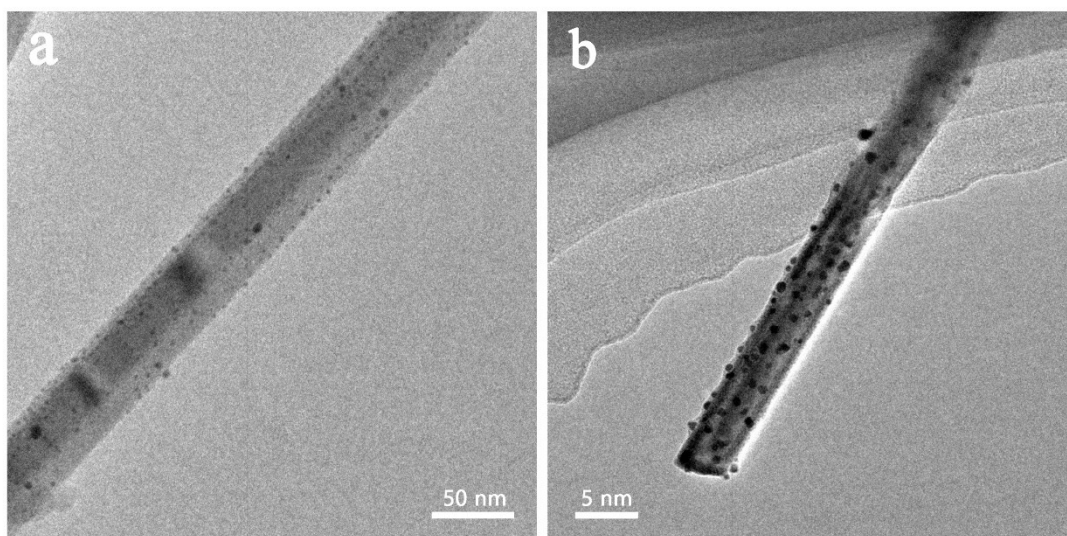


Fig. S11 The TEM images of Au/CdS@Au-S samples at Au addition of (a) 10% and (b) 4%.

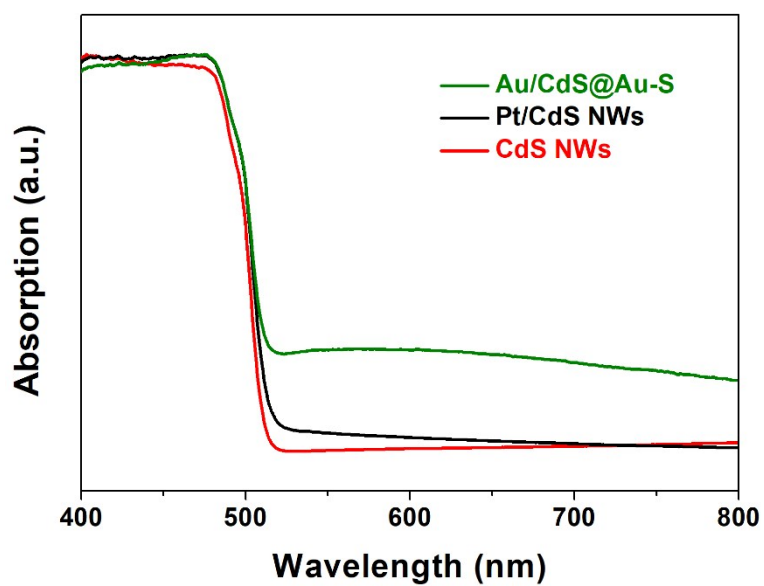


Fig. S12 The UV-Vis spectra of different photocatalysts.

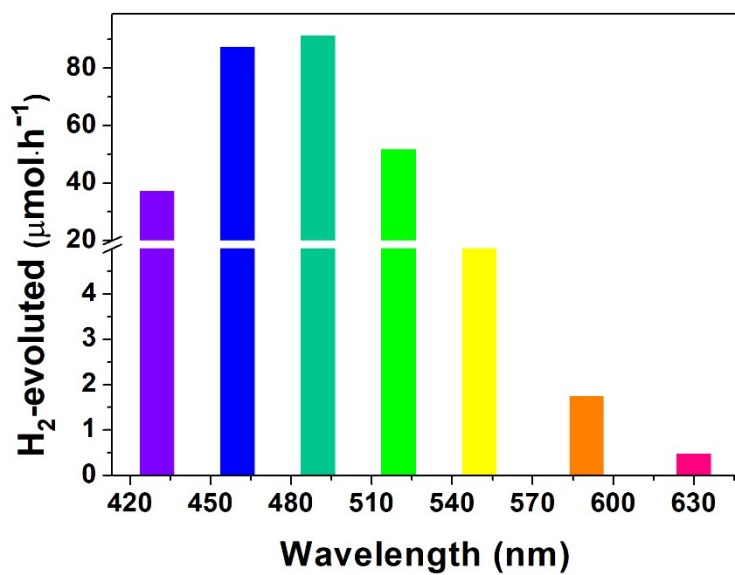


Fig. S13 Changes in hydrogen evolution activity under different wavelength light irradiations.

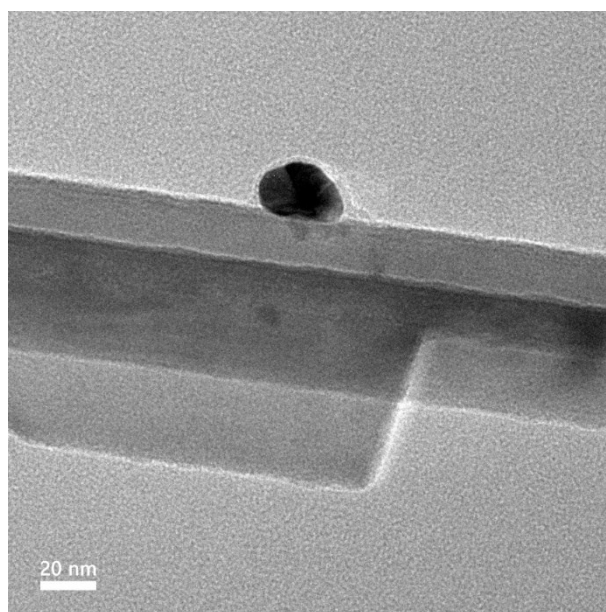


Fig. S14 The TEM image of Au/CdS@Au-S after photocatalytic reaction.

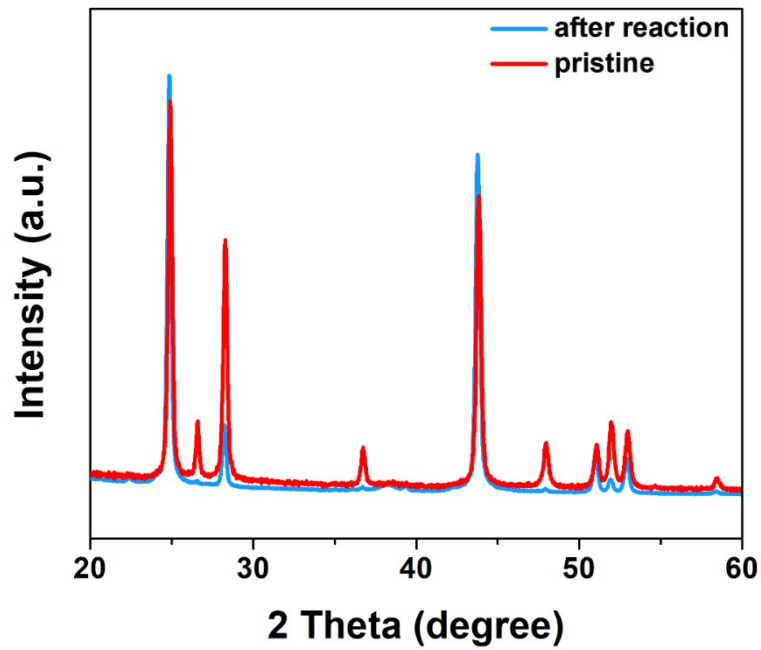


Fig. S15 The XRD patterns of Au/CdS@Au-S photocatalyst before and after photocatalytic reaction.

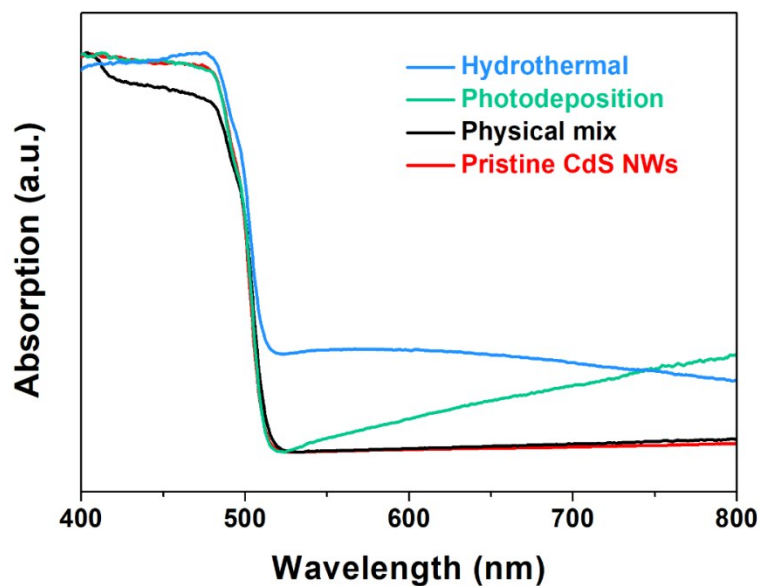


Fig. S16 The UV-vis spectra of Au combined CdS NWs photocatalysts via different route preparation.

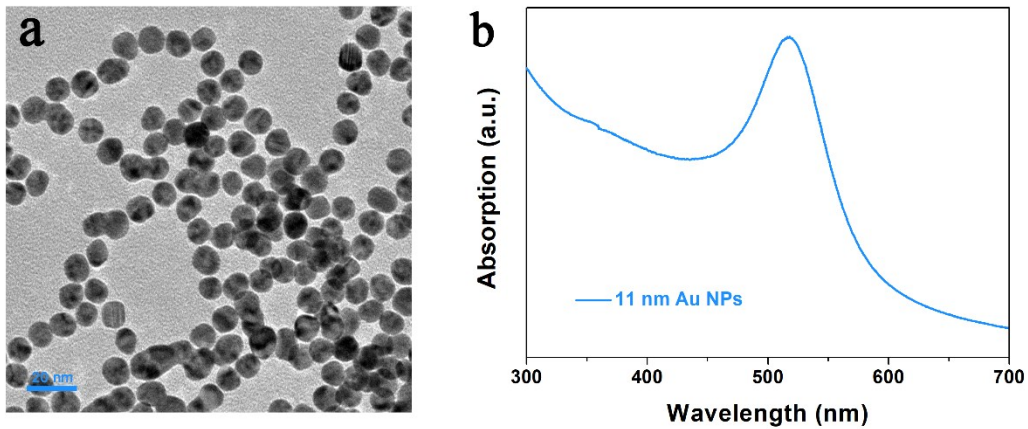


Fig. S17 (a) The TEM image and (b) UV-vis absorption spectrum of prepared Au NPs sol.

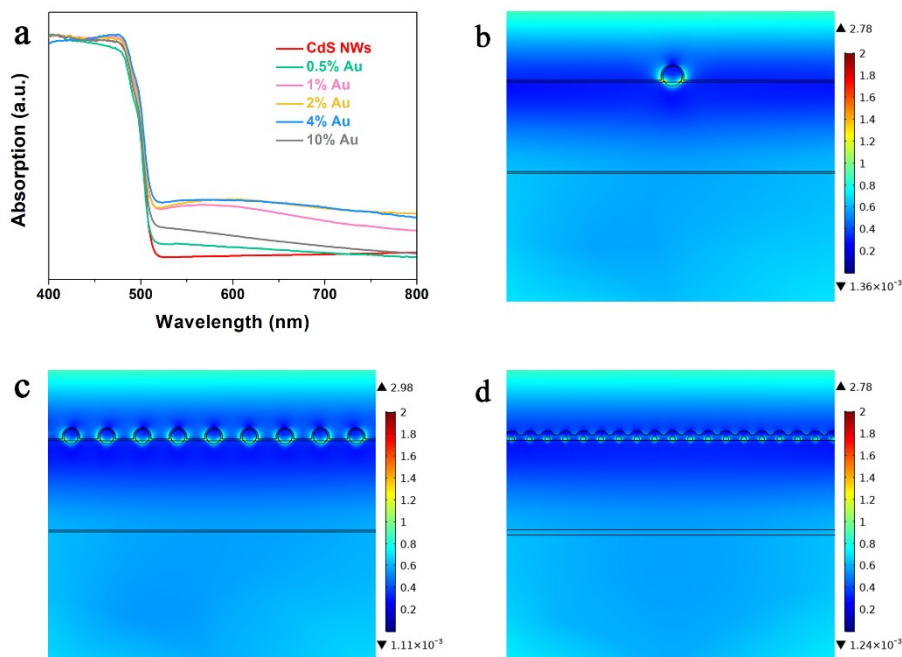


Fig. S18 Optical absorption and electromagnetic field simulation of photocatalysts. (a) The UV-vis spectra of Au/CdS@Au-S NWs photocatalysts with different Au addition amount. The electromagnetic field distributions on the surface of the Au/CdS@Au-S with Au addition amount of (b) 0.5%, (c) 4% and (d) 10%, respectively. The wavelength of the incident light was 520 nm.

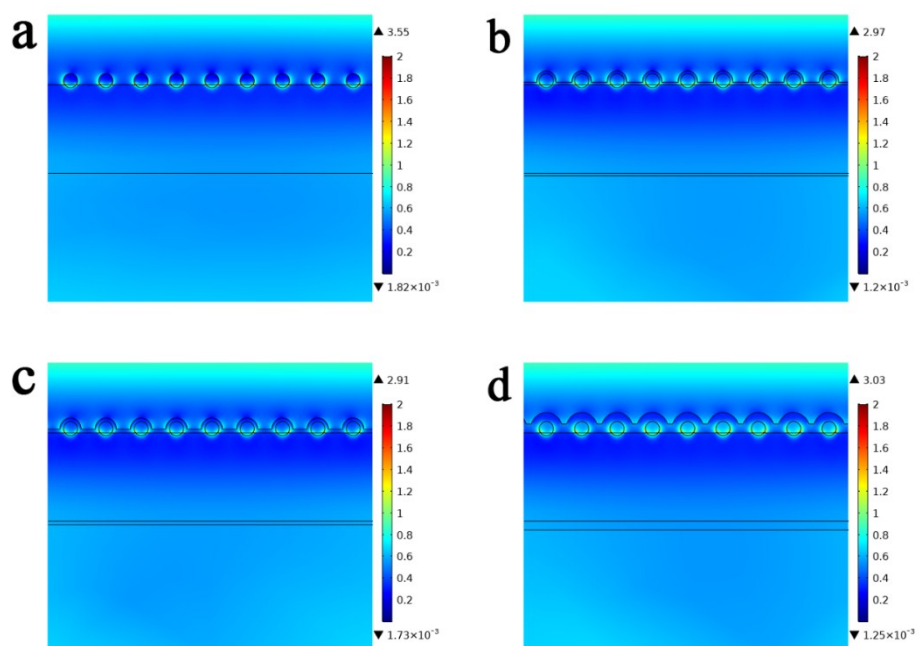


Fig. S19 Local electric field contours for Au/CdS@Au-S plasmonic nanocavities structures with different Au-S shell layer thickness: (a) 0 nm (bare Au/CdS NWs), (b) 1.5 nm, (c) 2.0 nm, and (d) 5.0 nm.

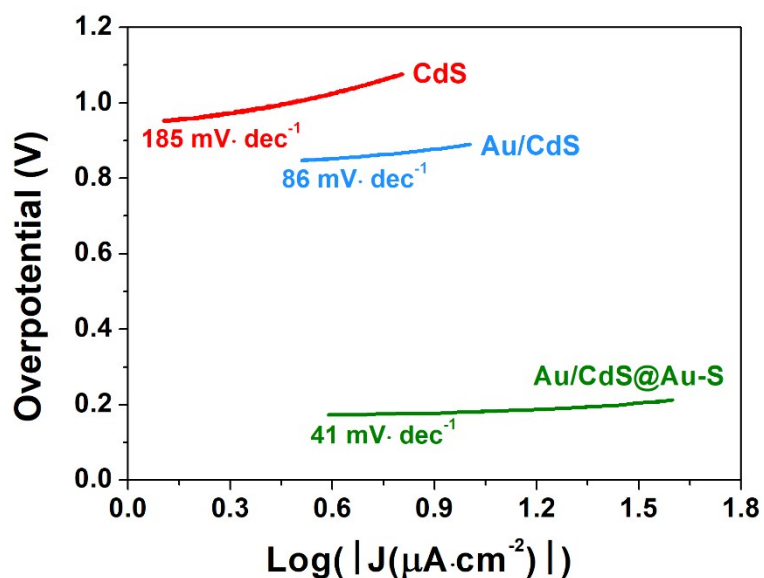


Fig. S20 The Tafel curves of different photocatalysts.

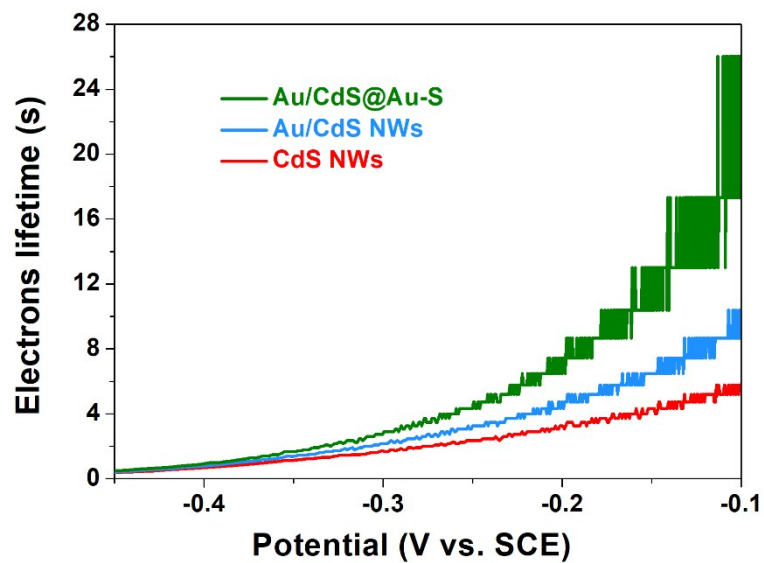


Fig. S21 The electrons lifetime determined from the decay of open circuit potential of bare CdS NWs, Au/CdS NWs and Au/CdS@Au-S photocatalysts.

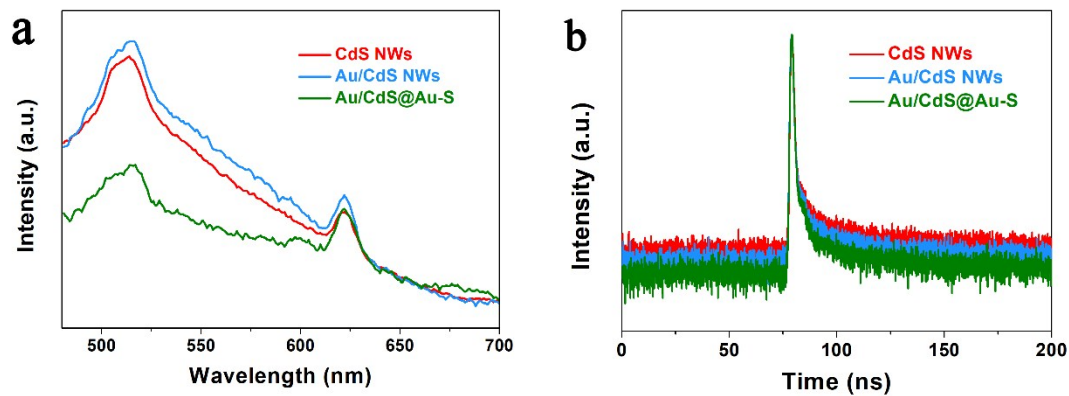


Fig. S22 (a) PL spectra of photocatalyst at room temperature, (b) TRPL spectra of photocatalyst and the excitation wavelength is 380 nm.

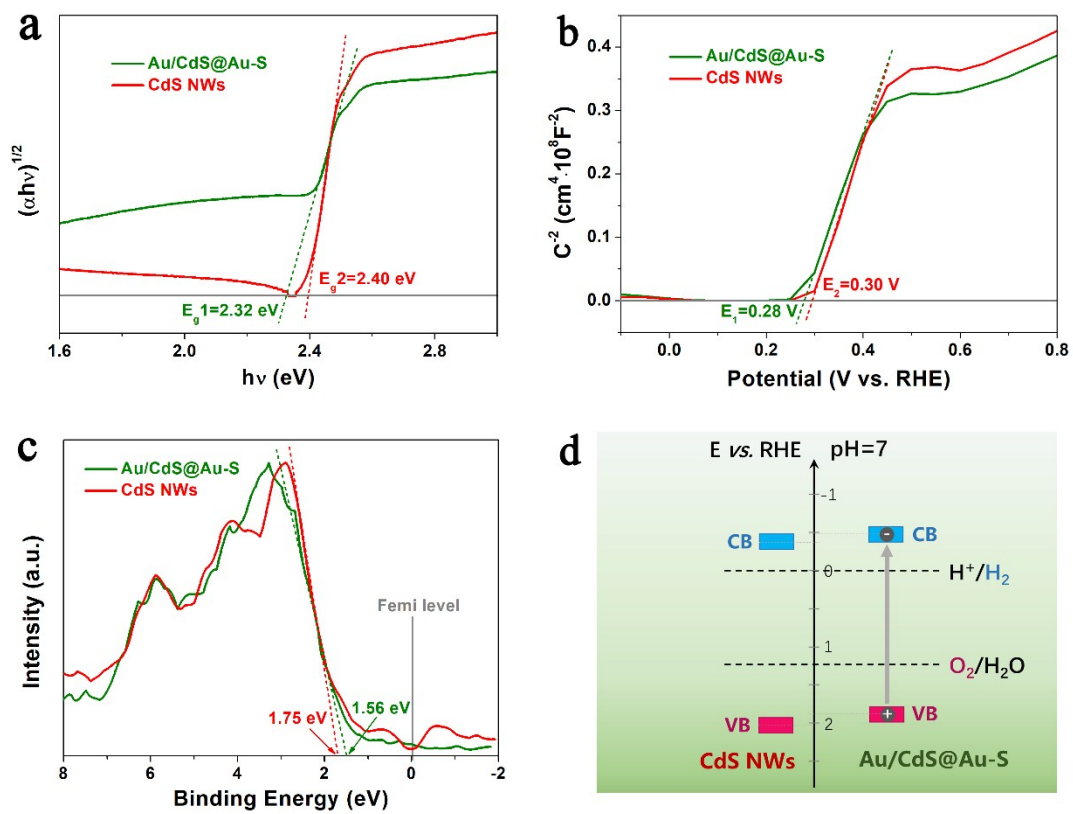


Fig. S23 (a) The band gap of catalyst, (b) the Mott-Schottky plots of catalyst, (c) the XPS valence spectra and (d) the band position from above results.

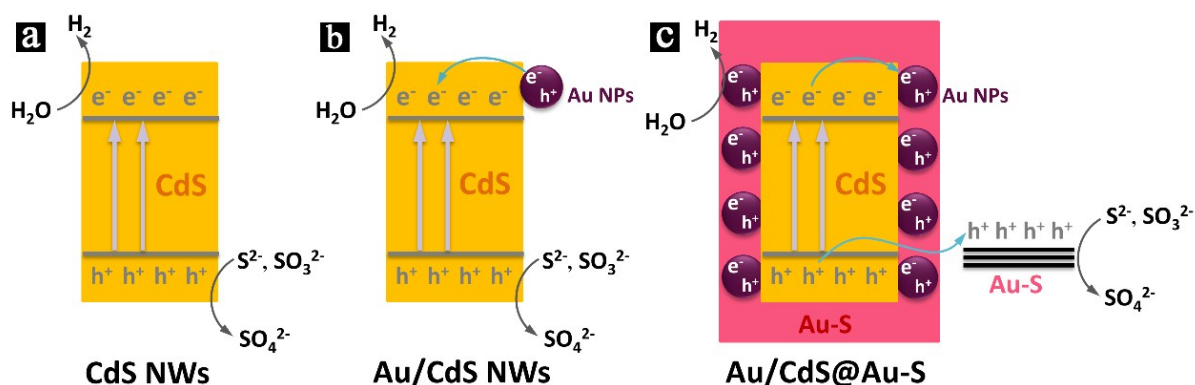


Fig. S24 The electron transfer process during photocatalytic reaction. In CdS system, as shown in Fig. S24a, it is a traditional photocatalytic mechanism. In Au/CdS system (Fig. S24b), the electron transfer process can be described as follow: under light irradiation ($\lambda > 420$ nm), both Au NPs and CdS NWs are excited, and the electron transfer to the CB of CdS NWs from Au NPs and the VB of CdS NWs, which can be confirmed our experiments and then the electrons react with **absorbed** H^+ to produce H_2 . The remaining holes will direct react with the pairs of Na_2S and Na_2SO_3 on the surface of CdS NWs. In Au/CdS@Au-S system (Fig. S24c), under visible light irradiation ($\lambda > 420$ nm), electrons are excited from the Au NPs and valence band (VB) of CdS NWs in Au/CdS@Au-S to the conduction band (CB) of CdS NWs, thereby forming the photogenerated electron-hole pairs. Simultaneously, the photogenerated positive holes, first are trapped by Au-S layer, and then quenched by scavenger (Na_2S and Na_2SO_3). On the other hand, due to the strong hole trapping ability of Au-S, to lead the rest of photogenerated electrons from CdS NWs can easily transfer to the Au NPs with a low lying Fermi level, by which the lifetime of photogenerated electrons is significantly improved. As a result, the adsorbed proton can be effectively reduced to hydrogen by accepting photogenerated electrons.^{S5,S6}

Tab. S1 The hydrogen production activity of CdS, Au/CdS and Au/CdS@Au-S under different light source irradiation.

<i>Catalysts</i>	<i>Conditions</i>	<i>Activity (μmol)</i>
CdS	$\lambda \leq 520 \text{ nm}$	33.9
	$\lambda > 520 \text{ nm}$	Undetected
Au/CdS@Au-S	$\lambda \leq 520 \text{ nm}$	1640.9
	$\lambda > 520 \text{ nm}$	10.2

Tab. S2 The hydrogen production activity and AQEs in recent papers.

<i>System</i>	<i>Conditions</i>	<i>Activity ($\mu\text{mol}\cdot\text{g}^{-1}\cdot\text{h}^{-1}$)</i>	<i>AQE/IPCE (%)</i>	<i>Ref.</i>
Au/CdS	10%, lactic acid, $\lambda > 420 \text{ nm}$	6385	2.4 at 420 nm	S7
Au@CdS	$0.1 \text{ mol}\cdot\text{L}^{-1} \text{ Na}_2\text{SO}_3 + 0.1 \text{ mol}\cdot\text{L}^{-1} \text{ Na}_2\text{S}$, $\lambda > 420 \text{ nm}$	383.6	N/A	S8
BP-Au-CdS	$0.35 \text{ mol}\cdot\text{L}^{-1} \text{ Na}_2\text{S} + 0.25 \text{ mol}\cdot\text{L}^{-1} \text{ Na}_2\text{SO}_3$, solar light	10100	5.3 at 420 nm	S9
Au-CdS/ZnS-RGO	$0.35 \text{ mol}\cdot\text{L}^{-1} \text{ Na}_2\text{S} + 0.25 \text{ mol}\cdot\text{L}^{-1} \text{ Na}_2\text{SO}_3$, $\lambda > 420 \text{ nm}$	9960	N/A	S10
Au-Pt-CdS	$0.35 \text{ mol}\cdot\text{L}^{-1} \text{ Na}_2\text{S} + 0.25 \text{ mol}\cdot\text{L}^{-1} \text{ Na}_2\text{SO}_3$, $\lambda > 420 \text{ nm}$	778	0.06 at 440 nm	S11
Au-CdS/ZnS	$0.35 \text{ mol}\cdot\text{L}^{-1} \text{ Na}_2\text{S} + 0.25 \text{ mol}\cdot\text{L}^{-1} \text{ Na}_2\text{SO}_3$, $\lambda > 400 \text{ nm}$	675	N/A	S12
NYF/Au/CdS	12%, ethanol, AM 1.5G	230	N/A	S13
Au/CdS	SO_3^{2-} and S^{2-} , $\lambda > 400 \text{ nm}$	7300	N/A	S14
CdS-Au-HCNS	3% Pt, 10% TEOA, $\lambda > 455 \text{ nm}$	13850	8.7 at 420 nm	S15
g-C ₃ N ₄ /Au/CdS	20%, lactic acid, $\lambda > 420 \text{ nm}$	1060	N/A	S16
Au/CdS@Au-S	$0.1 \text{ mol}\cdot\text{L}^{-1} \text{ Na}_2\text{SO}_3 + 0.1 \text{ mol}\cdot\text{L}^{-1} \text{ Na}_2\text{S}$, $\lambda > 420 \text{ nm}$	11000	19.1 at 430 nm	This work

References

- S1. I. Majeed, M. A. Nadeem, E. Hussain, A. Badshah, R. Gilani and M. A. Nadeem, *International Journal of Hydrogen Energy*, 2017, 42, 3006-3018.
- S2. J. J. Li, Y. A. Wang, W. Z. Guo, J. C. Keay, T. D. Mishima, M. B. Johnson and X. G. Peng, *Journal of the American Chemical Society*, 2003, 125, 12567-12575.
- S3. J. Liu, Y. Liu, N. Liu, Y. Han, X. Zhang, H. Huang, Y. Lifshitz, S.-T. Lee, J. Zhong and Z. Kang, *Science*, 2015, 347, 970-974.
- S4. B. Tian, W. Gao, X. Zhang, Y. Wu and G. Lu, *Applied Catalysis B-Environmental*, 2018, 221, 618-625.
- S5. S. Yu, X.-B. Fan, X. Wang, J. Li, Q. Zhang, A. Xia, S. Wei, L.-Z. Wu, Y. Zhou and G. R. Patzke, *Nature Communications*, 2018, 9.
- S6. Y. P. Xie, Z. B. Yu, G. Liu, X. L. Ma and H.-M. Cheng, *Energy & Environmental Science*, 2014, 7, 1895-1901.
- S7. J. Xu, W.-M. Yang, S.-J. Huang, H. Yin, H. Zhang, P. Radjenovic, Z.-L. Yang, Z.-Q. Tian and J.-F. Li, *Nano Energy*, 2018, 49, 363-371.
- S8. X. Ma, K. Zhao, H. Tang, Y. Chen, C. Lu, W. Liu, Y. Gao, H. Zhao and Z. Tang, *Small*, 2014, 10, 4664-4670.
- S9. X. Cai, L. Mao, S. Yang, K. Han and J. Zhang, *Acs Energy Letters*, 2018, 3, 932-939.
- S10. S. Kai, B. Xi, X. Liu, L. Ju, P. Wang, Z. Feng, X. Ma and S. Xiong, *Journal of Materials Chemistry A*, 2018, 6, 2895-2899.
- S11. L. Ma, K. Chen, F. Nan, J.-H. Wang, D.-J. Yang, L. Zhou and Q.-Q. Wang, *Advanced Functional Materials*, 2016, 26, 6076-6083.
- S12. T.-T. Zhuang, Y. Liu, M. Sun, S.-L. Jiang, M.-W. Zhang, X.-C. Wang, Q. Zhang, J. Jiang and S.-H. Yu, *Angewandte Chemie-International Edition*, 2015, 54, 11495-11500.
- S13. W. Feng, L. Zhang, Y. Zhang, Y. Yang, Z. Fang, B. Wang, S. Zhang and P. Liu, *Journal of Materials Chemistry A*, 2017, 5, 10311-10320.
- S14. Q. Zhao, M. Ji, H. Qian, B. Dai, L. Weng, J. Gui, J. Zhang, M. Ouyang and H. Zhu, *Advanced Materials*, 2014, 26, 1387-1392.

- S15. D. Zheng, C. Pang and X. Wang, *Chemical Communications*, 2015, 51, 17467-17470.
- S16. W. Li, C. Feng, S. Dai, J. Yue, F. Hua and H. Hou, *Applied Catalysis B-Environmental*, 2015, 168, 465-471.